

# Facile preparation of metal organic framework modified covalent organic framework for efficient dispersive solid-phase extraction of toxic basic dyes in food

Weidan Yang, Shaowei Wu, Lu Xu, Jie Pang\*, Zhiming Yan\*

College of Food Science, Fujian Agriculture and Forestry University, Fuzhou, 350002, China



## ARTICLE INFO

### Keywords:

Covalent organic frameworks  
Metal organic frameworks  
Dispersive solid-phase extraction  
Toxic basic dyes

## ABSTRACT

High performance adsorbents are crucial for improving the efficiency of sample pretreatment and ensuring the accuracy and precision of analytical results. In this study, covalent organic framework COF-SCU1 was modified with metal-organic framework ZIF-8 for efficient extraction of toxic basic dyes in food. The prepared COF-SCU1@ZIF-8 exhibited improved dispersibility and more surface negative charges compared to COF-SCU1, thereby showing enhanced adsorption performance for auramine O, rhodamine B, basic orange 21, basic orange 22 and methylene blue. The dispersive solid-phase extraction (D-SPE) for toxic basic dyes based on COF-SCU1@ZIF-8 consumed tiny amount of adsorbent and solvent as well as short operation time. An analytical method for the determination of toxic basic dyes was developed based on D-SPE and high-performance liquid chromatography with detection limits of 0.9–1.6 ng mL<sup>-1</sup>. The developed method was applied to the detection of toxic basic dyes in real food samples with recoveries of 88.20–105.83 %.

## 1. Introduction

Basic dyes such as auramine O (AO), rhodamine B (RB), basic orange 21 (B21), basic orange 22 (B22), and methylene blue (MB), are classified as synthetic cationic dyes. These dyes are extensively utilized in textiles, synthetic fibers, plastics, and leather due to affordability, durability, and intense coloring capabilities (Tan et al., 2024; Wang et al., 2023). However, they pose significant health risks to humans, including carcinogenicity, mutagenicity, allergic reactions, dermatitis, and kidney diseases (Dutta et al., 2021). Many countries and international food safety regulations strictly prohibit using AO, RB, B21, B22, and MB in food products (Lu et al., 2012; Tatebe et al., 2014). Hence, developing susceptible and effective detection methods for these toxic basic dyes in food is imperative to safeguard public health and ensure food safety.

Due to the low concentrations of basic dyes and matrix interference in food, it is crucial to employ sample preconcentration and purification steps before instrumental analysis to ensure precise detection. Extraction methods such as solid phase extraction (SPE) (Khalikova et al., 2014), liquid-liquid extraction (LLE) (Khan et al., 2019; Mortada, 2020), filled in-tube solid phase microextraction (FIT-SPME) (Nasrollahi et al., 2022), magnetic solid phase extraction (M-SPE) (Zhou et al., 2023) and D-SPE (Büyüktiryaki et al., 2020) are commonly employed for extraction

of basic dyes. D-SPE has benefits such as minimal solvent usage, rapid extraction times, and straightforward operation. The adsorbent in D-SPE is crucial for determining extraction efficiency, accuracy, and sensitivity of the analysis.

Covalent organic frameworks (COFs) are crystalline organic materials formed by covalent bonds between light elements such as H, O, C, N, B and Si, arranged in two-dimensional or three-dimensional porous structures. Metal organic frameworks (MOFs) are a type of porous material formed by coordination bonds between metal clusters and organic ligands (Parsapour et al., 2024; Shahid et al., 2024). COFs and MOFs are widely utilized in catalysis, sensors, gas storage, drug delivery and sample preparation due to high surface area, high porosity, and tunable structures (Amodu et al., 2024; Diercks & Yaghi, 2017; Maleki et al., 2024; Zhang, Zhou, et al., 2024). However, MOFs and COFs have inherent limitations that partially hinder their widespread application. For instance, MOFs have relatively weak coordination bonds, and in the presence of water, the organic ligands of MOFs can be gradually replaced by water molecules, leading to framework collapse. Furthermore, many COFs are characterized by small particle sizes and low density, presenting challenges in efficiently recovering of these materials in practical applications. Recent studies have shown that effectively integrating different types of MOFs and COFs materials not only retains

\* Corresponding authors.

E-mail addresses: [3721941@163.com](mailto:3721941@163.com) (J. Pang), [45765545@qq.com](mailto:45765545@qq.com) (Z. Yan).

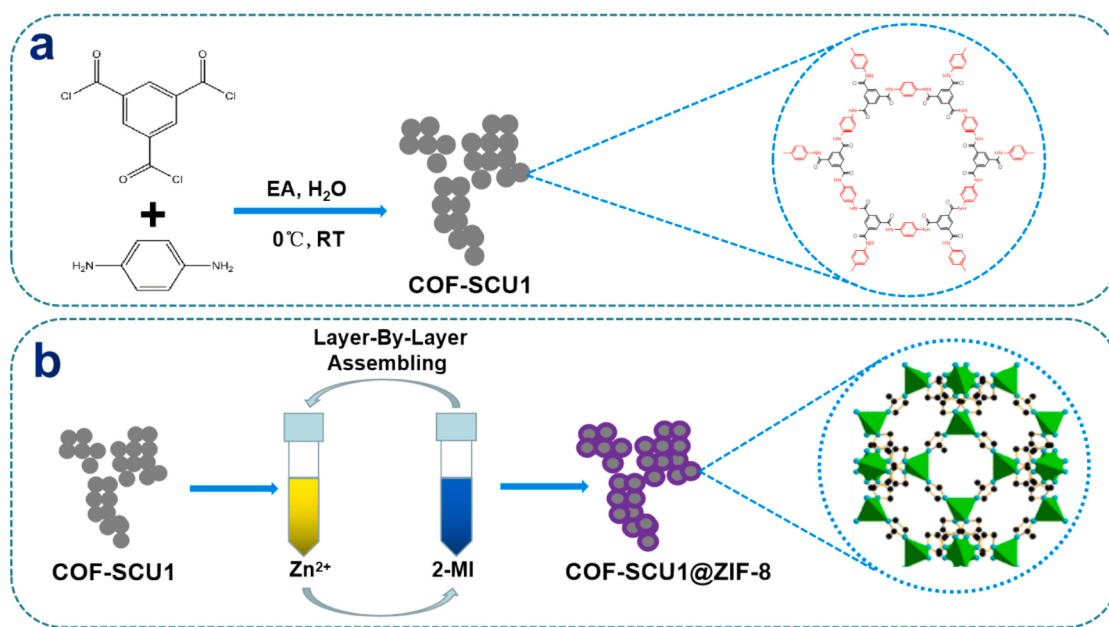


**Fig. 1.** Schematic diagram of synthesizing COF-SCU1 and COF-SCU1@ZIF-8.

their respective advantages but also mitigates their shortcomings, demonstrating excellent potential in various applications. For example, [Jiang et al. \(2021\)](#) reported the preparation of magnetic TAPB-COF@ZIF-8 composite for effective extraction of bisphenols. [Koonani and Ghiasvand \(2024\)](#) reported a Zn-MOF/COF composite for headspace solid phase extraction of polycyclic aromatic hydrocarbons (PAHs).

Herein, a novel COF@MOF composite with fast kinetics and large adsorption capacity for toxic basic dyes was reported for dispersive solid-phase extraction of basic dyes in food. COF-SCU1 is a carboxyl-rich two-dimensional COF, synthesized from the polymerization of trimesoyl chloride and *p*-phenylenediamine. COF-SCU1 could be considered as an potential adsorbent for effective extraction of basic dyes due to its abundance of carboxyl groups ([Li et al., 2015](#)). However, COF-SCU1 tends to aggregate during drying, which results in poor dispersion and a reduction of active adsorption sites, thereby limiting its overall adsorption performance ([Wang et al., 2020](#)). An effective strategy to address this issue is to modify COF-SCU1 with a functional coating to alter the interactions between particles and reduce the tendency to aggregate. ZIF-8 is a classic MOF with excellent characteristics such as high specific surface area, good chemical and thermal stability, and adjustable pore structure ([Saliba et al., 2018](#)). Particularly, ZIF-8 could be decorated onto various types of materials with versatile properties ([Ahmad et al., 2024](#); [Li et al., 2023](#); [Zhang, Sun, et al., 2024](#)). In this study, COF-SCU1 was modified with ZIF-8 to prepare COF-SCU1@ZIF-8 and overcome the aggregation issue of COF-SCU1. This study investigated the morphology, crystal structure, chemical properties, and adsorption performance of the prepared COF-SCU1@ZIF-8. Furthermore, the main factors affecting the extracting efficiency of basic dyes by COF-SCU1@ZIF-8 was systematically optimized. Finally, a D-SPE/HPLC method based on COF-SCU1@ZIF-8 was developed and applied to detect five toxic basic dyes in fish sauce, shrimp sauce, red wine and carbonated drink.

## 2. Material and methods

### 2.1. Materials

AO ( $\geq 80\%$ ), B21 ( $\geq 95\%$ ), B22 ( $\geq 95\%$ ), RB ( $\geq 97.1$ ) and MB ( $\geq 98.5\%$ ) were products of YuanYe Biotechnology (Shanghai, China), the chemical structures of five basic dyes are listed in Fig. S1; 1,3,5-

benzenetricarbonyl trichloride, 2-methylimidazole (2-MI), *p*-phenylenediamine, zinc nitrate, and ammonium acetate were procured from Sinopharm Chemical Reagent (Shanghai, China); Acetic acid and ethyl acetate (EA), chromatography-grade methanol and acetonitrile were supplied from Macklin Biochemical (Shanghai, China). Fish sauce, shrimp sauce, red wine and carbonated drink were purchased from local market in Fuzhou.

### 2.2. Instruments

Scanning electron microscope (SEM) and transmission electron microscope (TEM) images were taken on QUANTA250 (FEI, USA) and Talos F200X (Thermo Fisher, USA), respectively. The X-ray diffraction (XRD) patterns were obtained using a D8 Advance X-ray diffractometer (Bruker, Germany). Fourier-transform infrared (FT-IR) spectra were collected by using a Nicolet 5700 spectrophotometer (Thermo Fisher, USA). Thermo-gravimetric analysis (TGA) was performed on TGA Q500 (TA Instruments, USA). Nitrogen adsorption and desorption isotherms were determined using an ASAP 2460 porosimeter (Micromeritics, USA). Zeta potential measurements were carried out using a Litesizer 500 nanosizer (Anton Paar, Austria) over the pH range of 2–11. Samples concentration were performed using a CVE 3000 vacuum centrifugal concentrator (EYELA, Japan).

An Agilent 1260 HPLC system (Agilent Technologies, USA) with diode array detector and IVENS C18 column ( $250 \times 4.6 \text{ mm}, 5 \mu\text{m}$ ) was used to analyze the five basic dyes. The HPLC experiment utilized a binary gradient elution method with solvent A consisting of  $0.02 \text{ mol L}^{-1}$  ammonium acetate- $0.1\%$  acetic acid aqueous solution, and solvent B composed of 100 % acetonitrile. The HPLC separation gradient was: beginning with 10 % solvent B, it was increased to 40 % within 3.0 min, further raised to 60 % within 2.0 min, reached 80 % at 15.0 min, and returned to the initial proportion of solvent B over 3 min. All HPLC experiments were conducted at  $30^\circ\text{C}$  with a flow rate of  $1.0 \text{ mL min}^{-1}$ . The ultraviolet detection wavelengths for AO, B21, B22, RB, and MB are 431 nm, 452 nm, 501 nm, 545 nm, and 653 nm, respectively.

### 2.3. Synthesis

#### 2.3.1. Synthesis of COF-SCU1

COF-SCU1 was synthesized following the reported literature with

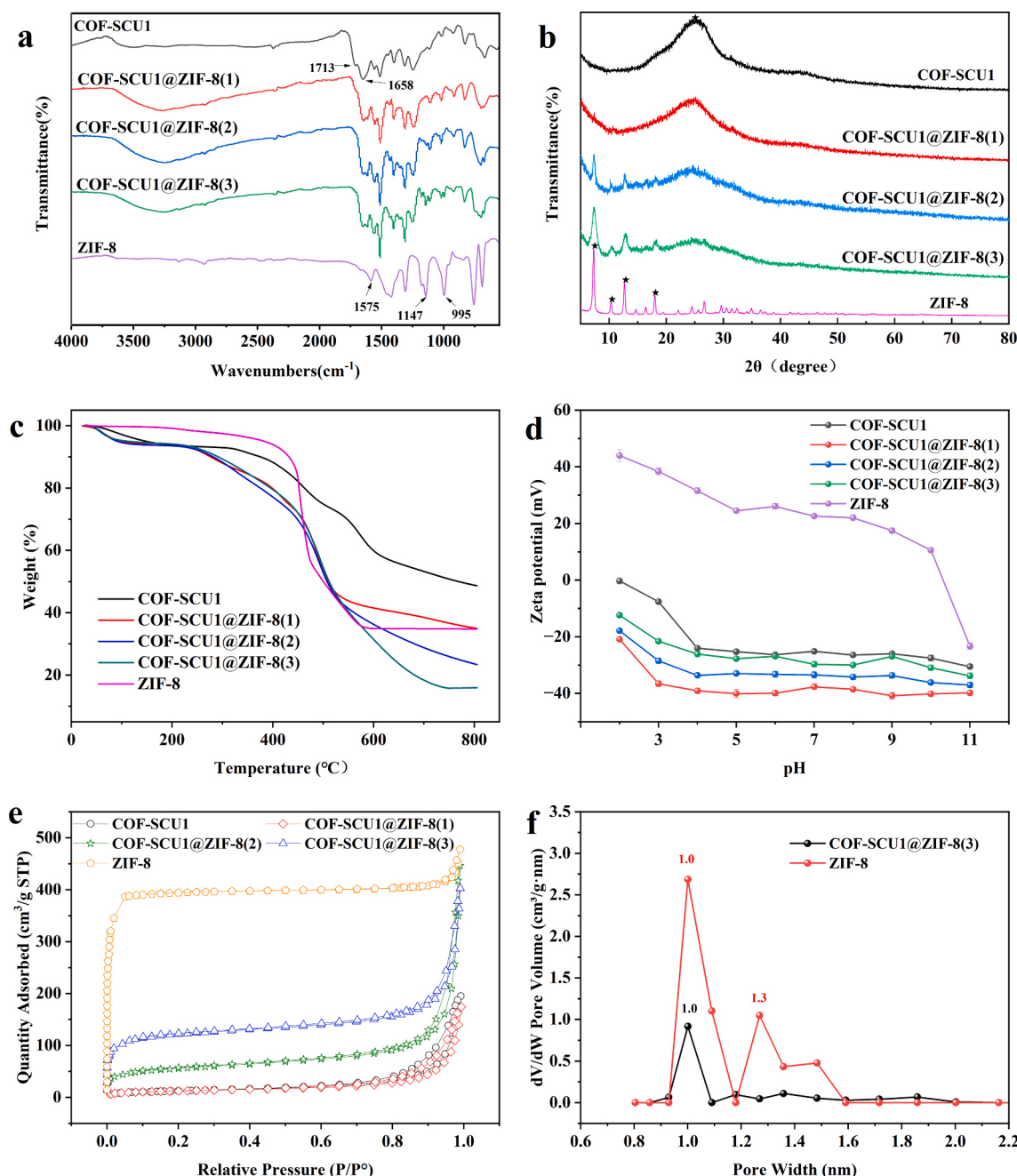


**Fig. 2.** (a) FT-IR spectra, (b) XRD patterns (c) TGA curves, (d) Zeta potentials and (e) nitrogen adsorption-desorption isotherms of COF-SCU1, COF-SCU1@ZIF-8(1), COF-SCU1@ZIF-8(2), COF-SCU1@ZIF-8(3) and ZIF-8; (f) pore size distribution of COF-SCU1@ZIF-8(3) and ZIF-8.

slight modifications (Wang et al., 2020), as illustrated in Fig. 1a. In brief, 2.12 g of 1,3,5-benzenetricarbonyl trichloride and 0.64 g of *p*-phenylenediamine were dissolved in 60 mL and 30 mL of EA, respectively. After placing the 1,3,5-benzenetricarbonyl trichloride solution in an ice-water bath, the *p*-phenylenediamine solution was added dropwise to the 1,3,5-benzenetricarbonyl trichloride solution within 1 h. Then, the mixture was incubated at room temperature for 24 h. Afterwards, the collected products were washed with water and ethanol, sequentially. Finally, the prepared COF-SCU1 was dispersed in water.

### 2.3.2. Synthesis of COF-SCU1@ZIF-8

COF-SCU1@ZIF-8 was synthesized via a layer-by-layer assembly strategy (Fig. 1b). Initially, 10 mL of COF-SCU1 suspension (38 mg mL<sup>-1</sup>) was combined with 5 mL of a ZnNO<sub>3</sub> aqueous solution (200 mg mL<sup>-1</sup>) and agitated for 30 min. After centrifugation to separate the

supernatant, the precipitate was then mixed with 5 mL of a methanol solution containing 2-MI (200 mg mL<sup>-1</sup>). The mixture was agitated for an additional 30 min. Then, the solid was collected by centrifuging and washed twice with methanol to complete one assembly cycle, resulting in the product named COF-SCU1@ZIF-8(1). The above procedure was repeated to achieve two and assembly cycles, resulting in products named COF-SCU1@ZIF-8(2) and COF-SCU1@ZIF-8(3), respectively. The obtained solid was dried under vacuum at 60 °C for 12 h before further experiments.

### 2.4. D-SPE procedure

The operational parameters of D-SPE were optimized using 50 ng mL<sup>-1</sup> standard solutions of AO, B21, B22, RB, and MB. The final procedure of D-SPE was optimized as follows: 1.0 mg of COF-SCU1@ZIF-8

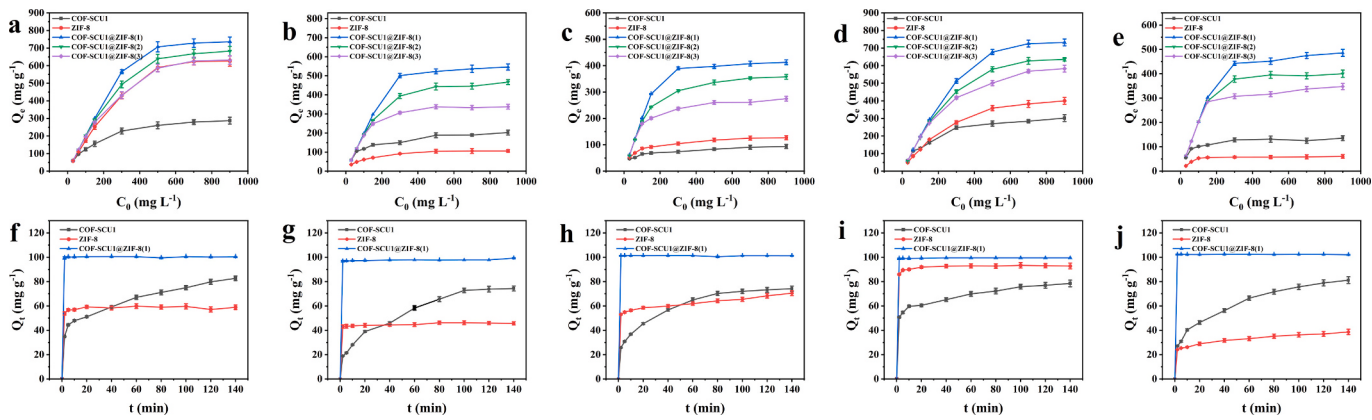


**Fig. 3.** (a-e) Adsorption isotherms of five toxic basic dyes on COF-SCU1, ZIF-8, COF-SCU1@ZIF-8(1), COF-SCU1@ZIF-8(2) and COF-SCU1@ZIF-8(3); (f-j) Adsorption kinetics of five toxic basic dyes on COF-SCU1, ZIF-8 and COF-SCU1@ZIF-8(1).

(1) was added to 10 mL of the sample solution and vortexed for 3 min to facilitate adsorption. After centrifuging the mixture, the supernatant was discarded while the resulting precipitate was then subjected to ultrasonication with 1 mL of 20 % formic acid-acetonitrile for 50 s. After centrifugation, the eluate was concentrated to dryness using vacuum centrifuge. It was subsequently reconstituted with 0.1 mL acetonitrile-water (1:1, v:v), filtered through a 0.22  $\mu$ m nylon membrane.

## 2.5. Preparation of real food samples

The preparation of fish and shrimp sauces samples followed the reported literature with some modifications (Sun et al., 2023). Typically, 2.0 g of homogenized sample was placed in a 50 mL centrifuge tube, adding 20 mL of 1 % acetonitrile/acetic acid and vortexed for 2 min. Then, the mixture was centrifuged, and the supernatant was frozen for 2 h to precipitate fat. Subsequently, the unfrozen solution was concentrated to 1 mL using vacuum centrifuge, and then set the volume to 20 mL with ultrapure water. Finally, the obtained solution was filtered and adjusted to pH 9.

For the red wine sample, it was centrifuged, filtered and adjusted to pH 9. For the carbonated drink sample, it was degassed using ultrasound for 15 min, filtered and adjusted to pH 9.

## 3. Results and discussion

### 3.1. Characterization of adsorbents

The morphologies of COF-SCU1 and COF-SCU1@ZIF-8 were investigated via SEM and TEM. The SEM image of COF-SCU1 showed that it appeared to be irregular sphere particles with significant aggregation (Fig. S2a). On the contrary, the SEM images of COF-SCU1@ZIF-8 demonstrated a notable improvement in the aggregation after modification of COF-SCU1 with ZIF-8 (Fig. S2b-d). It also observed from the TEM images of COF-SCU1 and COF-SCU1@ZIF-8(3) that the particle diameters increased after three assembly cycles (Fig. S2e, S2b). The energy dispersive X-ray spectrometry (EDX) mapping results revealed that only C, N and O elements were distributed in COF-SCU1 (Fig. S2f-j), while Zn element was also found in COF-SCU1@ZIF-8 besides C, N and O elements (Fig. S2n-q).

The FT-IR spectra of COF-SCU1, ZIF-8, and COF-SCU1@ZIF-8 were depicted in Fig. 2a. Characteristic peaks of COF-SCU1 at 1658 and 1713 cm<sup>-1</sup> were corresponded to amide bonds and carboxyl groups, respectively (Zhang et al., 2017). Furthermore, it could be seen from the FT-IR spectra of COF-SCU1@ZIF-8 that the carboxyl groups at 1713 cm<sup>-1</sup> was not observed after one assembly cycle. Meanwhile, the intensity of the amide bonds at 1658 cm<sup>-1</sup> decreased with increasing the number of assembly cycles. The above results indicated that the immobilization of

Zn<sup>2+</sup> onto COF-SCU1 in the modification of ZIF-8 was attributed to the coordination between the amide bonds and carboxyl groups of COF-SCU1 and Zn<sup>2+</sup>, respectively. Additionally, the characteristic peaks of ZIF-8 at 995, 1147, and 1575 cm<sup>-1</sup> could be observed in the FT-IR spectra of COF-SCU1@ZIF-8, and the intensity of these peaks gradually strengthened with increasing the number of assembly cycles. The FT-IR results demonstrated the successful modification of COF-SCU1 with ZIF-8.

To further validate the successful preparation of COF-SCU1@ZIF-8, crystal structures of COF-SCU1, ZIF-8, and COF-SCU1@ZIF-8 were characterized using XRD (Fig. 2b). The XRD pattern of COF-SCU1 exhibited a broad peak at  $2\theta = 26^\circ$ , indicating its amorphous structure. Furthermore, it could be observed that as the number of assembly cycles increased, the intensity of the amorphous peak of COF-SCU1 gradually decreased, while the intensity of the characteristic peaks of ZIF-8 at  $2\theta = 7.6^\circ, 10.6^\circ, 12.9^\circ$ , and  $18.1^\circ$  notably increased. The XRD results also reaffirmed the successful preparation of COF-SCU1@ZIF-8.

The thermal stability of COF-SCU1, ZIF-8, and COF-SCU1@ZIF-8 were evaluated using TGA (Fig. 2c). COF-SCU1 demonstrated good thermal stability, with only an 8 % weight loss at 300 °C and a final weight loss of 52 % at 800 °C. ZIF-8 experienced a weight loss of only 6 % at 400 °C, then a rapid weight loss to 66.2 % at 595 °C, after which it plateaued. The three COF-SCU1@ZIF-8 with different numbers of ZIF-8 layers showed similar thermal stability from 25 to 500 °C, with a weight loss of 53 % at 500 °C. However, they exhibited significant differences in thermal stability from 500 to 800 °C. COF-SCU1@ZIF-8(1), COF-SCU1@ZIF-8(2) and COF-SCU1@ZIF-8(3) experienced weight losses of 66 %, 77 %, and 84 % at 800 °C, respectively. It could be concluded that the thermal stability of ZIF-8 layer on COF-SCU1 was much worse than that of pure ZIF-8, and the thermal stability of COF-SCU1@ZIF-8 became worse with modifying more ZIF-8.

The zeta potentials of COF-SCU1, ZIF-8, and COF-SCU1@ZIF-8 were also investigated and illustrated in Fig. 2d. COF-SCU1 exhibited a negative charge in the pH range of 2–11, with an increase in negative surface charge as pH increased due to deprotonation of carboxyl groups of COF-SCU1. On the other hand, ZIF-8 showed a positive charge from pH 2 to 10, with decreasing potential as pH increased, turning negatively charged at pH 11. Additionally, the potentials of three COF-SCU1@ZIF-8 samples were all lower than that of COF-SCU1 across the pH range of 2 to 11. Specifically, COF-SCU1@ZIF-8 with one assembly cycle exhibited the lowest potential, with the potential of gradually increasing as the number of assembly cycles increased.

The porous properties of COF-SCU1, ZIF-8, and COF-SCU1@ZIF-8 were characterized by nitrogen adsorption-desorption. It could be observed from Fig. 2e that the adsorption-desorption isotherms of COF-SCU1 and ZIF-8 corresponded to Type IV and Type I isotherms, respectively. COF-SCU1@ZIF-8(1) exhibited a similar adsorption-

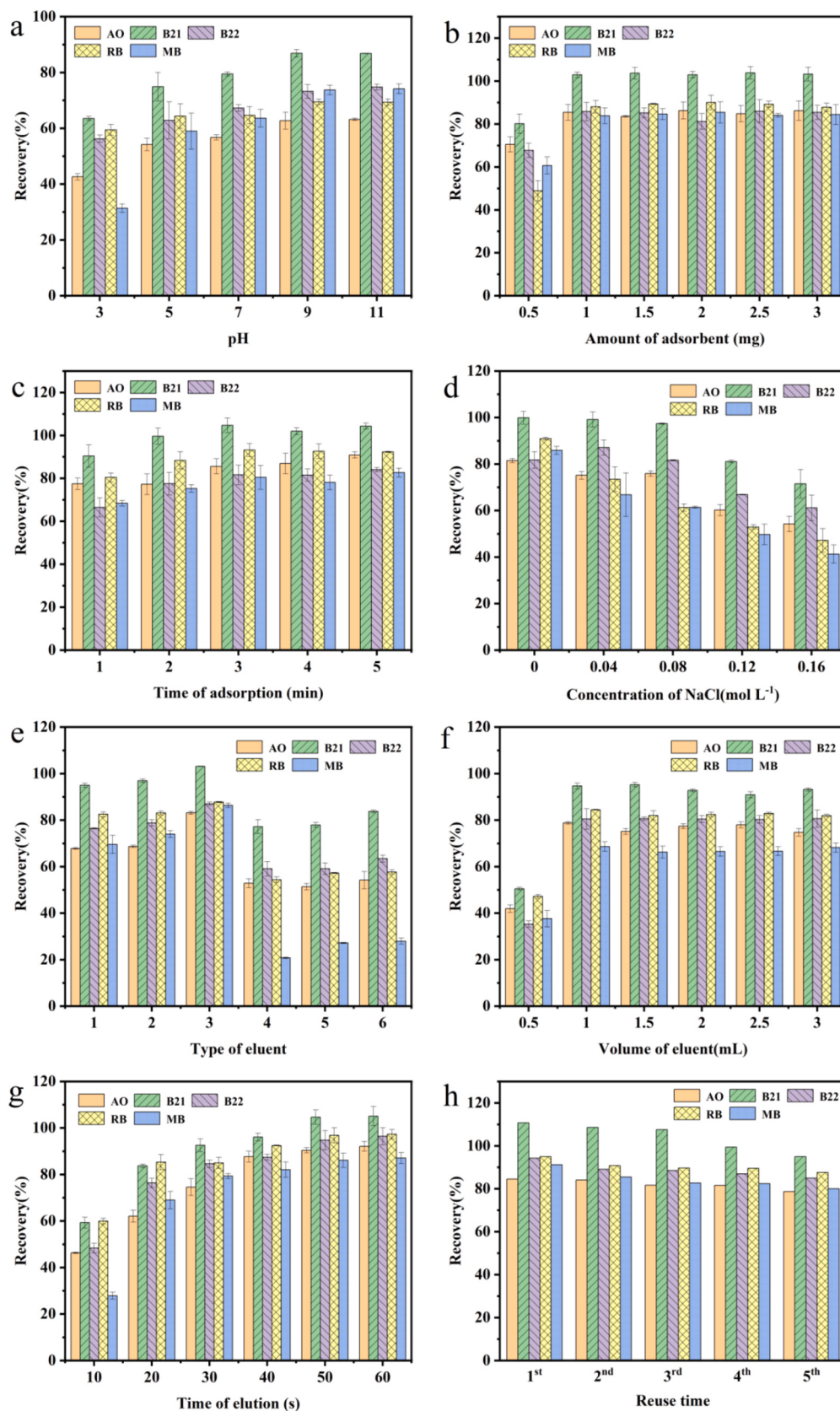


**Fig. 4.** Optimization of the D-SPE: (a) pH value; (b) COF-SCU1@ZIF-8 dosage; (c) time of adsorption; (d) concentration of NaCl; (e) type of eluent; 1:10 % formic acid-acetonitrile (v:v); 2: 15 % formic acid-acetonitrile (v:v); 3: 20 % formic acid-acetonitrile (v:v); 4: 10 % formic acid-methanol (v:v); 5: 15 % formic acid-methanol (v:v); 6: 20 % formic acid-methanol (v:v); (f) volume of eluent; (g) time of elution. (h) Reproducibility of COF-SCU1@ZIF-8.

desorption isotherm to COF-SCU1 with a pronounced hysteresis loop. However, the hysteresis loop of COF-SCU1 gradually diminished and the adsorption rate at low pressure significantly improved with increasing the number of assembly cycles. The Brunauer-Emmett-Teller (BET) surface areas of COF-SCU1 and ZIF-8 were calculated to be 45.62 and  $1656.48 \text{ m}^2 \text{ g}^{-1}$ , respectively. Furthermore, it could be observed that the assembly cycles significantly affect the BET surface areas of COF-SCU1@ZIF-8. Although the BET surface area of COF-SCU1@ZIF-8(1) was determined to be only  $45.40 \text{ m}^2 \text{ g}^{-1}$ , the BET surface areas of COF-SCU1@ZIF-8(2) and COF-SCU1@ZIF-8(3) rapidly increased to 204.0 and  $457.48 \text{ m}^2 \text{ g}^{-1}$ , respectively. As for the pore volume and pore characteristics (Table S1), COF-SCU1 was mesoporous with a pore volume of  $0.292 \text{ cm}^3 \text{ g}^{-1}$ , whereas ZIF-8 was primarily microporous with a pore volume of  $0.738 \text{ cm}^3 \text{ g}^{-1}$  and pore sizes of 1.0 and 1.3 nm (Fig. 2f). The pore volumes of COF-SCU1@ZIF-8(1) and COF-SCU1@ZIF-8(2) were 0.249 and  $0.689 \text{ cm}^3 \text{ g}^{-1}$ , respectively, both exhibited primarily mesoporous characteristics. While COF-SCU1@ZIF-8(3) exhibited a combined mesoporous and microporous structure with a total pore volume of  $0.62 \text{ cm}^3 \text{ g}^{-1}$ , including a micropore volume of  $0.15 \text{ cm}^3 \text{ g}^{-1}$  and a micropore size of 1.0 nm (Fig. 2f).

### 3.2. Evaluation the adsorption performance of adsorbents

The adsorption performance of COF-SCU1, ZIF-8, and COF-SCU1@ZIF-8 were evaluated using isothermal adsorption and adsorption kinetics experiments. Details of the adsorption kinetic and adsorption isothermal experiments are available in the supporting information. It can be observed from Fig. 3a-e that the adsorption capacities of the three COF-SCU1@ZIF-8 composites were all higher than those of COF-SCU1 and ZIF-8, and the adsorption capacities of COF-SCU1@ZIF-8 decreased with an increase in the assembly numbers. The isothermal adsorption data were fitted using Langmuir and Freundlich models (Table S2). The isothermal adsorption of COF-SCU1, ZIF-8, and COF-SCU1@ZIF-8 for basic dyes accorded with Langmuir model with higher correlation coefficients ( $R^2 > 0.99$ ). Furthermore, according to the Langmuir model, the calculated maximum adsorption capacities of COF-SCU1@ZIF-8(1) for AO, B21, B22, RB, and MB at 303 K were 714.3, 526.32, 400.01, 714.29 and  $476.2 \text{ mg g}^{-1}$ , which were 2.42, 2.74, 4.36, 2.43 and 3.71 times higher than COF-SCU1, and also 1.07, 5.1, 3.08, 1.64, and 9.62 times larger than ZIF-8, respectively.

Since COF-SCU1@ZIF-8(1) exhibited the best adsorption capacities for the five basic dyes, it was chosen for the adsorption kinetics. As could be seen from Fig. 3f-j, COF-SCU1@ZIF-8 exhibited very fast adsorption kinetics for basic dyes, reaching adsorption equilibrium within 2 min at dyes concentration of  $50 \text{ mg mL}^{-1}$ . In contrast, COF-SCU1 and ZIF-8 required more time to reach adsorption equilibrium. The adsorption kinetic data were fitted using pseudo-first-order and pseudo-second-order kinetic models (Fig. S3 and Table S3). It was found that the pseudo-second-order kinetic model exhibited a higher correlation coefficient ( $R^2 > 0.999$ ), and the theoretical equilibrium adsorption capacities were closer to the experimental equilibrium adsorption capacities.

The higher adsorption capacities and faster adsorption kinetics of COF-SCU1 after modifying with ZIF-8 could be attributed to two aspects. On the one hand, the dispersibility of COF-SCU1 was significantly improved after modifying with ZIF-8 (Fig. S4), providing more active adsorption sites and enhancing the adsorption performance for basic dyes. On the other hand, electrostatic interaction was crucial for the adsorption of basic dyes, and the modification of COF-SCU1 with ZIF-8 increased its negative charges (Fig. 2d), thereby improving the adsorption performance for basic dyes.

### 3.3. Optimization of D-SPE

The surface charge of adsorbent and the ionization of basic dyes are both pH-dependent, significantly impacting the extraction efficiency of

basic dyes. Therefore, the effect of solution pH ranging from 3 to 11 on recoveries of basic dyes was studied, as shown in Fig. 4a. The recoveries of the five basic dyes gradually increased as the pH increased from 3 to 9, and kept almost no change as further raising the pH to 11. Based on the chemical structures of five basic dyes, it's known that they were positively charged. COF-SCU1@ZIF-8 exhibited negative charges across the pH range of 3 to 11, with the negative charge gradually increasing from pH 3 to 9, which suggested that electrostatic interaction between COF-SCU1@ZIF-8 and basic dyes played a crucial role in the extraction of basic dyes. Therefore, the solution pH was adjusted to 9.

The effect of COF-SCU1@ZIF-8 dosage on the recoveries of basic dyes was studied ranging from 0.5 mg to 3.0 mg, as depicted in Fig. 4b, the recoveries of basic dyes exhibited a significant increase as the COF-SCU1@ZIF-8 dosage escalated from 0.5 mg to 1.0 mg. In addition, increasing the COF-SCU1@ZIF-8 dosage from 1 mg to 3 mg did not result in significantly improving the recoveries of basic dyes. Therefore, 1.0 mg of COF-SCU1@ZIF-8 was selected for subsequent experiments to ensure optimal recoveries of basic dyes.

During the extraction process, adsorption time is one of the most critical factors affecting the mass transfer rate of target analytes from the matrix to the adsorbent. Vortex can accelerate molecular mass transfer rates, thereby reducing equilibrium times. The influence of vortex adsorption time (1–5 min) on the recoveries of basic dyes was studied. From Fig. 4c, it could be seen that as the vortex adsorption time increased to 3 min, the recoveries of basic dyes significantly increased, subsequently reaching equilibrium. Therefore, 3 min of vortex adsorption time was chosen in the subsequent experiments.

The ionization and solubility of target analytes could be influenced by the ionic strength of the sample solution, thereby impacting their extraction efficiency. This study investigated the impact of ionic strength on basic dye recoveries by adding varying concentrations of NaCl (0–0.16 mol L<sup>-1</sup>) to the solution. According to Fig. 4d, it was evident that as the NaCl concentration increased, the recoveries of basic dyes gradually decreased. The addition of salt dismissed the electrostatic interaction between the basic dye and COF-SCU1@ZIF-8, thereby decreasing the extraction efficiency of basic dyes by COF-SCU1@ZIF-8. Consequently, there is no need to add NaCl to the sample solution.

The selection of eluent significantly impacts elution efficiency. Acidified methanol and acidified acetonitrile were evaluated as eluents in this study. As found in Fig. 4e, 20 % formic acid-acetonitrile (v:v) exhibited the highest elution efficiency among these selected eluents. Furthermore, the effect of elution volume was also examined, as depicted in Fig. 4f. The recoveries of five basic dyes significantly increased as the eluent volume increased from 0.5 to 1.0 mL, and kept stable as further expanding the eluent volume. Therefore, 1.0 mL of 20 % formic acid-acetonitrile (v:v) was selected for elution.

Elution time is a critical factor affecting D-SPE. The effect of ultrasonic elution time ranging from 10 to 60 s on the recoveries of basic dyes was investigated, as listed in Fig. 4g. The recoveries of basic dyes gradually improved as the ultrasonic elution time increased from 10 s to 50 s, and reached equilibrium after 50 s. Therefore, ultrasonic elution time of 50 s was selected in subsequent experiments.

### 3.4. Reusability of COF-SCU1@ZIF-8

The reusability of COF-SCU1@ZIF-8 was validated through five consecutive cycles of D-SPE. To ensure no residual basic dyes before the subsequent use, the used COF-SCU1@ZIF-8 was sequentially rinsed with 1 mL of methanol followed by 1.0 mL of ultrapure water. As shown in Fig. 4h, there was no significant decrease in recoveries after five cycles of D-SPE, demonstrating the excellent reusability of COF-SCU1@ZIF-8.

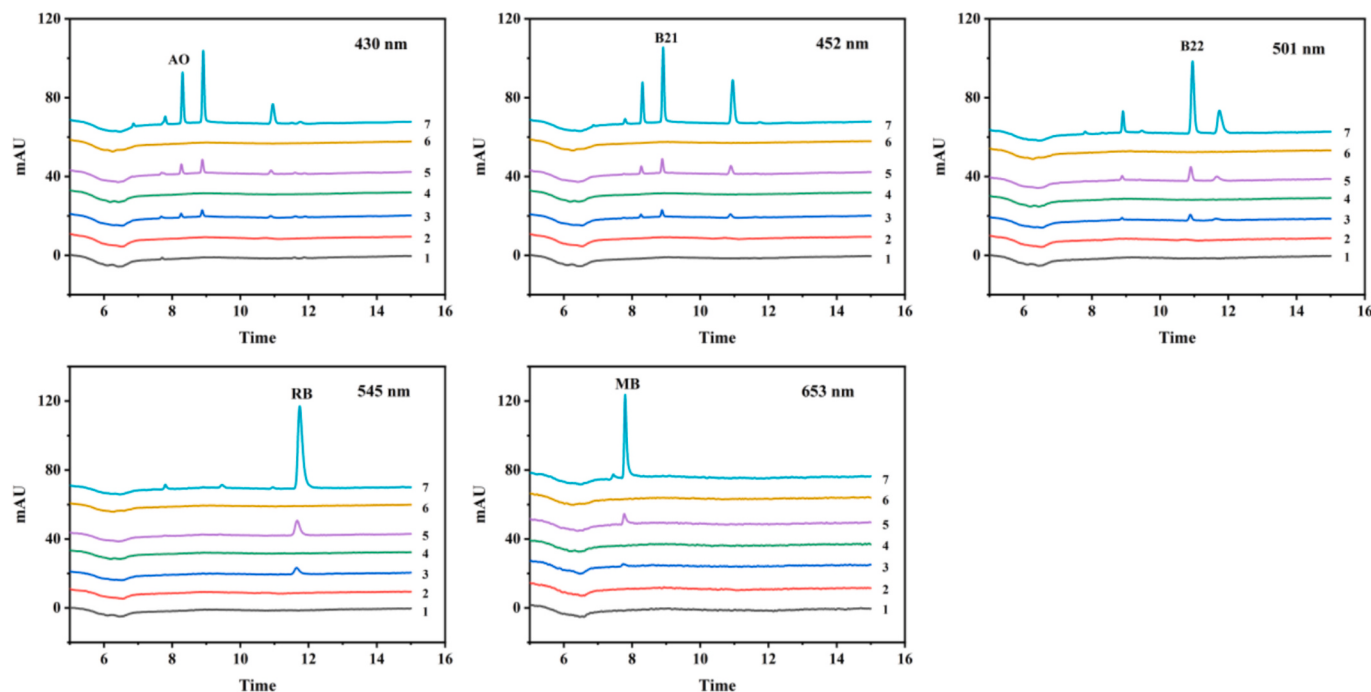
### 3.5. Evaluation of matrix effect

The matrix effect (ME) was evaluated by comparing the slope of the matrix-matched calibration curve and the slope of the solvent

**Table 1**

Results for the analysis of five toxic basic dyes in fish sauce, shrimp sauce, red wine and carbonated drink.

Analytes	Added (ng mL <sup>-1</sup> )	Fish sauce			Shrimp sauce			Red wine			Carbonated drink		
		Found (ng mL <sup>-1</sup> )	Recovery (%)	RSD (%)	Found (ng mL <sup>-1</sup> )	Recovery (%)	RSD (%)	Found (ng mL <sup>-1</sup> )	Recovery (%)	RSD (%)	Found (ng mL <sup>-1</sup> )	Recovery (%)	RSD (%)
AO	0	nd <sup>a</sup>											
	5	4.51	90.21	3.93	4.58	91.62	3.89	4.70	93.91	1.77	4.91	98.17	0.86
	10	9.75	97.54	1.97	9.50	95.05	2.81	9.19	91.92	1.99	9.39	93.88	1.29
	50	46.83	93.67	1.49	46.80	93.60	1.55	47.62	95.25	1.68	48.24	96.49	2.07
B21	0	nd <sup>a</sup>											
	5	5.29	105.83	2.93	5.04	100.71	2.03	4.91	98.25	2.51	4.81	96.29	2.58
	10	9.46	94.65	1.71	10.26	102.56	4.06	9.26	92.60	4.52	9.40	94.02	2.83
	50	50.32	100.63	1.42	46.60	93.20	2.64	48.96	97.93	2.81	46.77	93.54	3.66
B22	0	nd <sup>a</sup>											
	5	4.86	97.25	4.47	4.83	96.57	4.22	4.92	98.49	1.72	4.95	98.96	3.00
	10	9.64	96.44	4.02	9.30	93.05	4.65	9.70	97.02	1.29	9.48	94.82	4.50
	50	47.29	94.59	0.31	47.06	94.12	4.05	49.32	98.64	3.57	45.18	90.36	1.50
RB	0	nd <sup>a</sup>											
	5	4.67	93.44	0.38	4.91	98.18	3.67	4.68	93.66	0.75	4.98	99.70	1.75
	10	9.82	98.25	0.50	9.52	95.24	4.24	9.94	99.42	4.02	9.57	95.66	0.77
	50	47.18	94.36	1.85	44.84	89.68	3.15	48.32	96.64	2.90	48.67	97.35	0.50
MB	0	nd <sup>a</sup>											
	5	4.48	89.53	2.87	4.99	99.82	0.42	4.53	90.51	4.48	4.60	92.00	1.35
	10	9.36	93.57	1.04	9.78	97.79	3.18	9.31	93.11	3.59	9.47	94.66	4.08
	50	48.40	96.81	1.61	44.10	88.20	1.50	47.81	95.62	2.63	48.54	97.07	2.83

nd<sup>a</sup>: not detected.**Fig. 5.** The chromatograms of (1) actual fish sauce with D-SPE; (2) spike fish sauce at 5 ng mL<sup>-1</sup> without D-SPE; (3) spike fish sauce at 5 ng mL<sup>-1</sup> with D-SPE; (4) spike fish sauce at 10 ng mL<sup>-1</sup> without D-SPE; (5) spike fish sauce at 10 ng mL<sup>-1</sup> with D-SPE; (6) spike fish sauce at 50 ng mL<sup>-1</sup> without D-SPE; (7) spike fish sauce at 50 ng mL<sup>-1</sup> with D-SPE.

calibration curve (Table S4). The ME values of AO, RB, B21, B22 and MB in fish sauce, shrimp sauce, red wine and carbonated drink samples were in the range of 90.82–108.78 %, indicated that appeared to be a certain degree of ME. Therefore, the current study employed matrix-matched calibration curves for the determination of five toxic basic dyes in food.

### 3.6. Method evaluation

To assess the validity of the proposed D-SPE/HPLC-UV method in quantifying five toxic basic dyes, various parameters including the linear range, regression equations, correlation coefficients, detection limits

(LOD) ( $S/N = 3$ ), quantification limits (LOQ) ( $S/N = 10$ ), and precision were examined, detailed in Table S5. The linear ranges for the five toxic basic dyes spanned from 3.0 to 400 ng mL<sup>-1</sup>, with correlation coefficients ( $R^2$ ) exceeding 0.999. The LOD and LOQ ranged between 0.9 and 1.6 ng mL<sup>-1</sup> and 3.0 to 5.3 ng mL<sup>-1</sup>, respectively. The intra-day and inter-day relative standard deviations (RSD) of the method were below 5.7 % and 5.9 %, respectively.

### 3.7. Analysis of real food samples

The proposed COF-SCU1@ZIF-8 based D-SPE/HPLC method was

employed to analyze five toxic basic dyes in samples of fish sauce, shrimp paste, red wine, and carbonated drink. The results showed that none of the five toxic basic dyes were detected in any of the four real food samples (Table 1). To further evaluate the reliability of the proposed analytical method, spiked tests were conducted on the four real food samples at spiked concentrations of 5, 10 and 50 ng mL<sup>-1</sup>. It could be found that the recoveries of the five toxic basic dyes in the four spiked samples ranged from 88.20 % to 105.83 %, with RSD ranging from 0.31 % to 4.56 %. The proposed method demonstrated strong reliability and accuracy in detecting five toxic basic dyes in samples of fish sauce, shrimp sauce, red wine, and carbonated drink. Fig. 5 showed the HPLC chromatograms of fish sauce sample after D-SPE as well as the spiked fish sauce samples before and after D-SPE. Additionally, the HPLC chromatograms of shrimp sauce, red wine and carbonated drink samples were shown in Fig. S5–7.

### 3.8. Methods comparison

The proposed COF-SCU1@ZIF-8 based D-SPE/HPLC method in quantifying of basic dyes was compared with previously reported methods regarding adsorbent dosage, adsorption time and LOD (Fang et al., 2013; Long et al., 2016; Qi et al., 2016; Sheibani et al., 2024; Shojaei et al., 2023; Yu et al., 2024), as shown in Table S6. It's evident that the proposed method offered advantages such as lower adsorbent dosage, shorter adsorption times or lower LOD. The above comparison results indicated that the proposed COF-SCU1@ZIF-8 based D-SPE/HPLC method in quantifying of five toxic basic dyes in food was very robust and highly practical.

## 4. Conclusion

In summary, a novel COF@MOF composite COF-SCU1@ZIF-8 was synthesized via a layer-by-layer assembly method for the first time. The prepared COF-SCU1@ZIF-8 exhibited better adsorption performance for AO, RB, B21, B22 and MB than parent COF-SCU1 and ZIF-8, which was primarily attributed to the improved dispersibility and more surface negative charges. The COF-SCU1@ZIF-8 based D-SPE procedure for extraction of basic dyes exhibited advantages such as short operation time, minimal adsorbent and solvent usage, and high extraction efficiency. The proposed D-SPE/HPLC method had been successfully applied to detect trace amounts of five toxic basic dyes in fish sauce, shrimp sauce, red wine, and carbonated drink with ideal sample recoveries and low RSD values. Nevertheless, the synthesis process of COF-SCU1@ZIF-8 in this study was relatively complex and time-consuming, and the influence of matrix effects on the analytical results was also not negligible. After the improvement of the synthesis process and the enhancement of selectivity, the application of COF@MOF composites in food analysis will also become increasingly widespread.

## CRediT authorship contribution statement

**Weidan Yang:** Writing – original draft, Investigation. **Shaowei Wu:** Investigation. **Lu Xu:** Investigation. **Jie Pang:** Writing – review & editing, Supervision. **Zhiming Yan:** Writing – review & editing, Supervision, Resources.

## Declaration of competing interest

The authors declare that they have no known competing financial interests or personal relationships that could have appeared to influence the work reported in this paper.

## Acknowledgement

This work was supported by the National Natural Science Foundation of China (grant no. 31801640), the Natural Science Foundation of Fujian

Province (grant no. 2023J01077), the Special Fund for Science and Technology Innovation of Fujian Agriculture and Forestry University (grant no. KFB23133).

## Appendix A. Supplementary data

Supplementary data to this article can be found online at <https://doi.org/10.1016/j.foodchem.2025.143728>.

## Data availability

Data will be made available on request.

## References

- Ahmad, K., Nde, D., Khan, R., & Raza, W. (2024). Fabrication of Zeolitic imidazolate framework-8 (ZIF-8) modified screen-printed electrode and its catalytic role for the electrochemical determination of biological molecule (dopamine). *Colloids and Surfaces A: Physicochemical and Engineering Aspects*, 699, Article 134606. <https://doi.org/10.1016/j.colsurfa.2024.134606>
- Amodu, I., Raimi, M., Ogbogu, M., Benjamin, I., Gulack, A., Adeyinka, A., & Louis, H. (2024). Mn-doped covalent organic framework (COF), graphene, and their nanocomposite (Mn@COF/CP) as sensors for oil-dissolved gases in transformer: A computational study. *Materials Today Communications*, 38, Article 108363. <https://doi.org/10.1016/j.mtcomm.2024.108363>
- Büyüktiryaki, S., Keçili, R., & Hussain, C. (2020). Functionalized nanomaterials in dispersive solid phase extraction: Advances & prospects. *TrAC Trends in Analytical Chemistry*, 127, Article 115893. <https://doi.org/10.1016/j.trac.2020.115893>
- Diercks, C., & Yaghi, O. (2017). The atom, the molecule, and the covalent organic framework. *Science*, 355(6328), 923–930. <https://doi.org/10.1126/science.aal1585>
- Dutta, S., Gupta, B., Srivastava, S., & Gupta, A. (2021). Recent advances on the removal of dyes from wastewater using various adsorbents: A critical review. *Materials Advances*, 2, 4497–4531. <https://doi.org/10.1039/dlma00354b>
- Fang, G., Wu, Y., Dong, X., Liu, C., He, S., & Wang, S. (2013). Simultaneous determination of banned acid orange dyes and basic orange dyes in foodstuffs by liquid chromatography-tandem electrospray ionization mass spectrometry via negative/positive ion switching mode. *Journal of Agricultural and Food Chemistry*, 61 (16), 3834–3841. <https://doi.org/10.1021/jf400619y>
- Jiang, H., Fu, Q., Wang, M., Lin, J., & Zhao, R. (2021). Determination of trace bisphenols in functional beverages through the magnetic solid-phase extraction with MOF-COF composite. *Food Chemistry*, 345, Article 128841. <https://doi.org/10.1016/j.foodchem.2020.128841>
- Khalikova, M., Šatinský, D., Šmidrková, T., & Solich, P. (2014). On-line SPE-UHPLC method using fused core columns for extraction and separation of nine illegal dyes in chilli-containing spices. *Talanta*, 130, 433–441. <https://doi.org/10.1016/j.talanta.2014.07.038>
- Khan, M., Khan, J., & Alqadami, A. (2019). A simple solvent extraction and ultra-performance liquid chromatography-tandem mass spectrometric method for the identification and quantification of rhodamine B in commercial lip balm samples. *Spectrochimica Acta Part a-Molecular and Biomolecular Spectroscopy*, 206, 72–77. <https://doi.org/10.1016/j.saa.2018.07.093>
- Koonani, S., & Ghasvand, A. (2024). A highly porous fiber coating based on a Zn-MOF/COF hybrid material for solid-phase microextraction of PAHs in soil. *Talanta*, 267, Article 125236. <https://doi.org/10.1016/j.talanta.2023.125236>
- Li, J., Yang, X., Bai, C., Tian, Y., Li, B., Zhang, S., & Li, S. (2015). A novel benzimidazole-functionalized 2-D COF material: Synthesis and application as a selective solid-phase extractant for separation of uranium. *Journal of Colloid and Interface Science*, 437, 211–218. <https://doi.org/10.1016/j.jcis.2014.09.046>
- Li, S., Thiagarajan, D., & Lee, B. (2023). Efficient removal of methylene blue from aqueous solution by ZIF-8-decorated helicoidal electrospun polymer strips. *Chemosphere*, 333, Article 138961. <https://doi.org/10.1016/j.chemosphere.2023.138961>
- Long, Z., Xu, W., Lu, Y., & Qiu, H. (2016). Nanosilica-based molecularly imprinted polymer nanoshell for specific recognition and determination of rhodamine B in red wine and beverages. *Journal of Chromatography B, Analytical Technologies in the Biomedical and Life Sciences*, 1029, 230–238. <https://doi.org/10.1016/j.jchromb.2016.06.030>
- Lu, Q., Gao, W., Du, J., Zhou, L., & Lian, Y. (2012). Discovery of environmental rhodamine B contamination in paprika during the vegetation process. *Journal of Agricultural and Food Chemistry*, 60(19), 4773–4778. <https://doi.org/10.1021/jf300067z>
- Maleki, B., Esmaili, H., Venkatesh, Y., & Yusuf, M. (2024). A critical review on MOFs and COFs-based heterogeneous catalysts in biodiesel generation: Synthesis methods, structural features, mechanisms, kinetic, economic/environmental evaluation, and their performance. *Process Safety and Environmental Protection*, 187, 903–925. <https://doi.org/10.1016/j.psep.2024.04.144>
- Mortada, W. I. (2020). Recent developments and applications of cloud point extraction: A critical review. *Microchemical Journal*, 157, Article 105055. <https://doi.org/10.1016/j.microc.2020.105055>
- Nasrollahi, S., Yamini, Y., & Mani-Varnosfaderani, A. (2022). A green approach for in-tube solid phase microextraction of acidic red dyes from juice samples using

- chitosan/poly vinyl alcohol electrospun nanofibers. *Journal of Food Composition and Analysis*, 106, Article 104339. <https://doi.org/10.1016/j.jfca.2021.104339>
- Parsapour, F., Moradi, M., Safarifard, V., & Sojdeh, S. (2024). Polymer/MOF composites for metal-ion batteries: A mini review. *Journal of Energy Storage*, 82, Article 110487. <https://doi.org/10.1016/j.est.2024.110487>
- Qi, P., Liang, Z., Wang, Y., Xiao, J., Liu, J., Liu, J., & Zhang, X. (2016). Mixed hemimicelles solid-phase extraction based on sodium dodecyl sulfate-coated nanomagnets for selective adsorption and enrichment of illegal cationic dyes in food matrices prior to high-performance liquid chromatography-diode array detection detection. *Journal of Chromatography A*, 1437, 25–36. <https://doi.org/10.1016/j.chroma.2016.02.005>
- Saliba, D., Ammar, M., Rammal, M., Al-Ghoul, M., & Hmudeh, M. (2018). Crystal growth of ZIF-8, ZIF-67, and their mixed-metal derivatives. *Journal of the American Chemical Society*, 140(5), 1812–1823. <https://doi.org/10.1021/jacs.7b11589>
- Shahid, M., Najam, T., Islam, M., Hassan, A., Assiri, M., Rauf, A., & Nazir, M. (2024). Engineering of metal organic framework (MOF) membrane for waste water treatment: Synthesis, applications and future challenges. *Journal of Water Process Engineering*, 57, Article 104676. <https://doi.org/10.1016/j.jwpe.2023.104676>
- Sheibani, M., Ghaedi, M., Zare-Shahabadi, V., Anaraki-Ardakani, H., & Asfaram, A. (2024). Ultrasound assisted solid phase extraction of methylene blue dye by MgSiO<sub>3</sub> nanoparticles through central composite design. *International Journal of Environmental Analytical Chemistry*, 104(13), 3142–3162. <https://doi.org/10.1080/03067319.2022.2078199>
- Shojaei, S., Rahmani, M., Khajeh, M., & Abbasian, A. (2023). Ultrasound assisted based solid phase extraction for the preconcentration and spectrophotometric determination of malachite green and methylene blue in water samples. *Arabian Journal of Chemistry*, 16(8), Article 104868. <https://doi.org/10.1016/j.arabjc.2023.104868>
- Sun, W., Xu, Q., Liu, Q., Wang, T., & Liu, Z. (2023). Post-synthetic modification of a magnetic covalent organic framework with alkyne linkages for efficient magnetic solid-phase extraction and determination of trace basic orange II in food samples. *Journal of Chromatography A*, 947, Article 463777. <https://doi.org/10.1016/j.chroma.2023.463777>
- Tan, L., Cao, Y., Yan, J., Mao, K., Liu, L., Wang, X., & Zhang, H. (2024). TiO<sub>2</sub> nanorod arrays@PDA/ag with biomimetic polydopamine as binary mediators for duplex SERS detection of illegal food dyes. *Analytica Chimica Acta*, 1287, 342047. <https://doi.org/10.1016/j.aca.2023.342047>
- Tatebe, C., Zhong, X., Ohtsuki, T., Kubota, H., Sato, K., & Akiyama, H. (2014). A simple and rapid chromatographic method to determine unauthorized basic colorants (rhodamine B, auramine O, and pararosaniline) in processed foods. *Food Science & Nutrition*, 2(5), 547–556. <https://doi.org/10.1002/fsn3.127>
- Wang, C., Lu, W., Song, W., Zhang, Z., Xie, C., Ji, Z., & Wang, J. (2023). Dual application of a cyano-containing covalent organic framework: Photocatalytic degradation of dyes with fluorescence detection studies. *Applied Catalysis A: General*, 666, Article 119433. <https://doi.org/10.1016/j.apcata.2023.119433>
- Wang, R., Li, C., Li, Q., Zhang, S., Lv, F., & Yan, Z. (2020). Electrospinning fabrication of covalent organic framework composite nanofibers for pipette tip solid phase extraction of tetracycline antibiotics in grass carp and duck. *Journal of Chromatography A*, 1622, Article 461098. <https://doi.org/10.1016/j.chroma.2020.461098>
- Yu, Y., Zhang, R., Hao, L., Li, Y., Wang, B., & Ge, D. (2024). Magnetic ZIF-8 extraction using supramolecular solvent based on ferrofluid and vortex-assisted liquid-liquid microextraction of cationic dyes in beverage and river water samples. *Microchemical Journal*, 109689. <https://doi.org/10.1016/j.microc.2023.109689>
- Zhang, J., Zhou, M., Mao, B., Huang, B., Wen, H., & Ren, J. (2024). The construction of COFs functionalized CRISPR electrochemical sensor for ultrasensitive detection of bacteria by hyper-branched rolling circle amplification. *Sensors and Actuators B: Chemical*, 409, Article 135610. <https://doi.org/10.1016/j.snb.2024.135610>
- Zhang, M., Sun, Y., Zhou, X., Yang, K., Sun, L., Qi, C., & Zhang, M. (2024). ZIF-8 decorated au/Al<sub>2</sub>O<sub>3</sub> hybrid material for highly selective hydrogenation of cinnamaldehyde. *Chemical Engineering Journal*, 479, Article 147595. <https://doi.org/10.1016/j.cej.2023.147595>
- Zhang, S., Yang, Q., Li, Z., Wang, W., Wang, C., & Wang, Z. (2017). Covalent organic frameworks as a novel fiber coating for solid-phase microextraction of volatile benzene homologues. *Analytical and Bioanalytical Chemistry*, 409(13), 3429–3439. <https://doi.org/10.1007/s00216-017-0286-x>
- Zhou, W., Wang, X., Liu, Y., Zhang, W., & Di, X. (2023). Novel Cu<sup>2+</sup>-based immobilized metal affinity magnetic nanoparticles for fast magnetic solid-phase extraction of trace Sudan dyes in food samples. *Food Chemistry*, 404, Article 134432. <https://doi.org/10.1016/j.foodchem.2022.134432>